



Share Your Innovations through JACS Directory

# Journal of Advanced Physical Sciences

Visit Journal at [www.jacsdirectory.com/japs](http://www.jacsdirectory.com/japs)

## Carbothermal Synthesis and Photoluminescence Characteristics of Pure Undoped ZnTiO<sub>3</sub> Nanocrystals

R.S. Raveendra<sup>1,2</sup>, P.A. Prashanth<sup>1,\*</sup>, R. Hari Krishna<sup>3</sup>, N.P. Bhagya<sup>1</sup>, S. Sathyanarayani<sup>1</sup>, B.M. Nagabhushana<sup>3</sup><sup>1</sup>Research Center, Department of Chemistry, Sai Vidya Institute of Technology, Bengaluru – 560 064, Karnataka, India.<sup>2</sup>Research and Development Centre, Bharathiar University, Coimbatore – 641 046, Tamil Nadu, India.<sup>3</sup>Department of Chemistry, M.S. Ramaiah Institute of Technology, Bengaluru – 560 054, Karnataka, India.

### ARTICLE DETAILS

#### Article history:

Received 26 October 2016

Accepted 14 November 2016

Available online 06 December 2016

#### Keywords:

Carbothermal  
Photoluminescence  
Optoelectronics  
Optical Band Gap

### ABSTRACT

ZnTiO<sub>3</sub> nanocrystals were synthesized by carbothermal synthesis using Zn(NO<sub>3</sub>)<sub>2</sub> and CO(NH<sub>2</sub>)<sub>2</sub> as starting materials. Powder X-ray diffraction (PXRD), Fourier transform infrared spectroscopy (FTIR), scanning electron microscopy (SEM), energy-dispersive X-ray spectroscopy (EDAX), high resolution transmission electron microscopy (HR-TEM) and UV-Vis absorption spectroscopy were used to characterize ZnTiO<sub>3</sub> nanocrystals. PXRD results shows that as-formed powder was amorphous and the hexagonal phase ZnTiO<sub>3</sub> nanocrystals forms after annealing the samples at temperature 800 °C for 2 hours. The optical band gap calculated from the absorption spectra using Tauc relation shows that the ZnTiO<sub>3</sub> has band gap of ~3.6 eV. Upon 345 nm excitation, the photoluminescence emission spectra shows number of emission peaks ranging from blue to green. The observed peaks are centered at 412, 450, 461, 471, 492, and 542 nm. These are attributed to the different kinds of vacancies such as oxygen defects and cation vacancies.

### 1. Introduction

With thriving growth on nanomaterials, the latest revolution in nanoscience, engineering, and technology is being driven by our capacity to manipulate matter to produce “designer” structures [1]. The mesoporous materials are regarded as designable nanomaterials. Since the discovery of ordered mesoporous silica materials in 1992 [2], this research field has been widely deliberated because of the possible applications of these materials as supports for catalysts and other areas in chemistry [3]. The ordered mesoporous materials give not just large surface areas, but also well uniform channels, narrow pore size distribution, and tunable pore sizes over an appreciably wide range. In the current days, great interest has been focused on the mesoporous metal oxides due to their potential application in various areas in electronic, photocatalytic, photovoltaic, and energy storage applications [4].

Compared with usual incandescent and fluorescent lamps, white light-emitting diodes (LEDs) as the lighting sources have received much more consideration, since they have the advantages of low energy consumption, reliability, high luminous efficiency, long lifetime and environmental protection. As of now, the most common method to get white light is combining a blue GaN chip with a yellow-emitting phosphor YAG: Ce<sup>3+</sup> [5–9]. However, there are several drawbacks in the practical application, including poor color-rendering index (Ra<80) owing to the deficiency of red emission and low luminous efficiency [10–12]. Therefore, some red phosphors are needed to lead into the combination. Unfortunately, commercially red phosphors for white LEDs such as Y<sub>2</sub>O<sub>2</sub>S:Eu<sup>3+</sup> show lower efficiency and chemical instability under NUV or blue light excitations [13]. Thus it is immediately required to seek substitute red phosphors with brilliant performance for white LEDs.

ZnTiO<sub>3</sub> is an inorganic compound, which can find applications in many fields such as white pigment and catalytic sorbent [14–16]. However, there has not been much work on the preparation of ZnTiO<sub>3</sub> nanocrystals especially by carbothermal commonly called solution combustion synthesis (SCS) method. In an earlier article, we reported the preparation, characterization, adsorption of dye and antibacterial activity of Nano ZnTiO<sub>3</sub> ceramics by SCS method for the first time [17]. It has been

demonstrated that ZnTiO<sub>3</sub> can also be considered as a promising luminescent material. ZnTiO<sub>3</sub> nanocrystals which can be used as white pigment and catalytic sorbents for the desulfurization of hot coal gases have attracted a good deal of attention [18]. Recent work has demonstrated that it can also be used as dielectric materials for microwave device and more preferably for low-temperature co-fired ceramics [19]. To our knowledge, photoluminescence (PL) of ZnTiO<sub>3</sub> has been reported in a very small number. In this view we decided to investigate the ZnTiO<sub>3</sub> nanocrystal as a potential PL material.

### 2. Experimental Methods

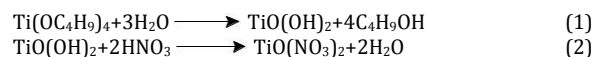
#### 2.1 Materials

Commercially available pure zinc nitrate hexahydrate (Zn(NO<sub>3</sub>)<sub>2</sub>·6H<sub>2</sub>O, AR 99%, Merck), tetra-n-butyl titanate (Ti(OC<sub>2</sub>H<sub>5</sub>)<sub>4</sub>, AR 99%, Aldrich), urea (CO(NH<sub>2</sub>)<sub>2</sub>, AR 99%, Merck), 1:1 nitric acid (HNO<sub>3</sub>, Fisher Scientific) are used as such without any further purification.

#### 2.2 Synthesis of ZnTiO<sub>3</sub> Nanocrystals

Carbothermal commonly known as solution combustion synthesis method was used synthesize ZnTiO<sub>3</sub> nanocrystals. In this method, the reaction mixture was calculated based on the total oxidizing and reducing valances of the oxidizer and fuel required to release the maximum energy for the reaction [20–22].

Firstly the titanyl nitrate solution was prepared by controlled hydrolysis of tetra n-butyl titanate with distilled water, further reaction of formed titanyl hydroxide with 1:1 HNO<sub>3</sub> gives titanyl nitrate. The following reactions occur during the formation.

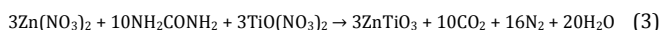


Formed titanyl nitrate was dissolved in little quantity water and the stoichiometric quantities of Zn(NO<sub>3</sub>)<sub>2</sub>, and CO(NH<sub>2</sub>)<sub>2</sub> were mixed in the distilled water and stirred well using a magnetic stirrer for about 20 min. The crystalline dish containing the; above solution was introduced into preheated muffle furnace maintained at 500±10 °C. The solution was boiled and resulted in a highly viscous liquid. This viscous liquid catches

\*Corresponding Author

Email Address: prsnthmysore@gmail.com (P.A. Prashanth)

fire and auto ignited with flames on the surface, which rapidly proceeded throughout the entire volume forming a white powdered product. The overall reaction can be written as,



The product formed was heated at 600 to 800 °C for 2 hours.

### 3. Results and Discussion

#### 3.1 Characterization Techniques

The product was characterized by PXRD. Powder X-ray diffraction patterns were collected on a Shimadzu XRD-700 X-ray Diffractometer with  $\text{CuK}\alpha$  radiation with diffraction angle range  $2\theta = 20^\circ$  to  $80^\circ$ . Product was morphologically characterized by FE-SEM performed on a ZEISS scanning electron microscope equipped with EDS. HR-TEM analysis which was performed on a Hitachi H-8100. The FT-IR studies have been performed on a Perkin Elmer Spectrometer (Spectrum 1000) with KBr pellet technique in the range of  $400\text{--}4000\text{ cm}^{-1}$ . To calculate optical energy band gap, UV-Vis spectrum was recorded using Elico SL-159 UV-Vis spectrophotometer.

#### 3.2 PXRD Studies

The formation of crystalline phase of synthesized product was confirmed by PXRD measurements. The PXRD of the product calculated at 800 °C for 2 hours is shown in the Fig. 1. All the peaks are in well agreement with the ICDD card number 26-1500 with a space group R-3 (No-148) and cell parameters  $a = b = 5.078\text{ \AA}$ ,  $c = 13.927\text{ \AA}$ . All the diffraction peaks can be indexed to (1 0 1), (1 0 2), (1 0 4), (1 1 0), (1 1 3), (0 2 4), (1 1 6), (0 1 8), (2 1 4), (3 0 0), (2 0 8), (1 1 9), (2 1 7) and (2 2 0) reflections. The broadening of the reflections clearly indicates the inherent nature of nanocrystals. The crystal structure of the  $\text{ZnTiO}_3$  nanocrystals is shown in Fig. 2. The crystallite size is calculated from the full width at half maximum (FWHM ( $\beta$ )) of the diffraction peaks using Debye-Scherrer's method [23] using the following equation,

$$d = \frac{k\lambda}{\beta \cos \theta} \quad (4)$$

where 'd' is the average crystalline dimension perpendicular to the reflecting phases, ' $\lambda$ ' is the X-ray wavelength, 'k' is shape factor, ' $\beta$ ' is the full width at half maximum (FWHM) intensity of a Bragg reflection excluding instrumental broadening and ' $\theta$ ' is the Bragg's angle. The calculated average crystallite size of the sample is found to be in the range of 15–20 nm.

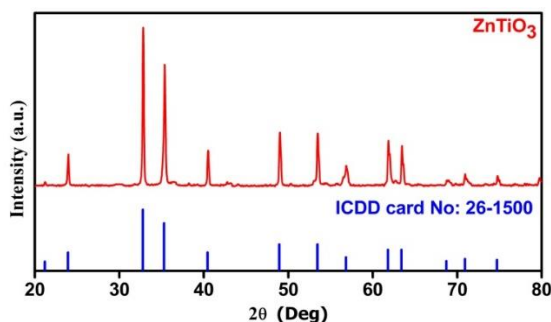


Fig. 1 PXRD patterns of  $\text{ZnTiO}_3$  nanocrystals

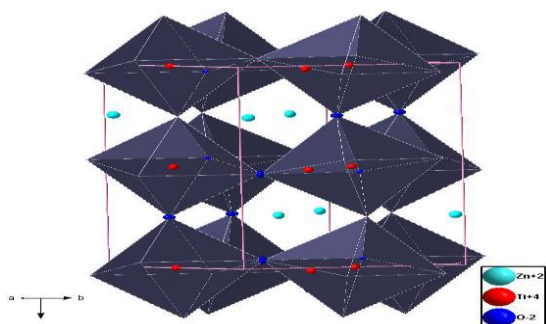


Fig. 2 Crystal structure of  $\text{ZnTiO}_3$  nanocrystals

#### 3.3 FT-IR Spectroscopic Studies

Fig. 3 shows the FT-IR spectrum of the  $\text{ZnTiO}_3$  nanocrystals recorded to define the vibrational frequency of metal-oxygen and other bonds related to impurities. It can be seen that no major impurity peaks corresponding to the organic impurities were observed. Strong absorption bands at  $570\text{ cm}^{-1}$  and  $410\text{ cm}^{-1}$  can be assigned to the stretching vibration of M-O bonds ( $\text{M} = \text{Zn}, \text{Ti}$ ) [24].

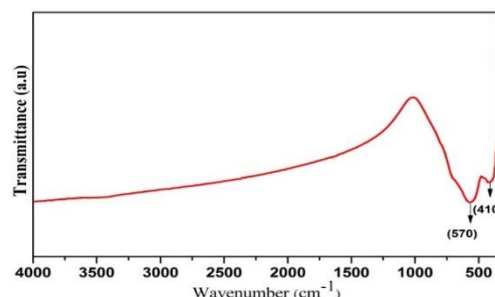


Fig. 3 FTIR spectrum of  $\text{ZnTiO}_3$  nanocrystals

#### 3.4 UV-Vis Spectroscopy Studies

To determine the optical energy band gap of  $\text{ZnTiO}_3$  nanocrystals, the UV-Vis absorption spectrum was recorded. The sample shows a strong absorption peak ( $\lambda_{\text{max}}$ ) at 235 nm at the UV region. Fig. 4a shows the UV-Vis absorption spectrum. This can be attributed to photo excitation of electron from valence band to conduction band. The optical energy band gap ( $E_g$ ) was estimated (Fig. 4b) by the method proposed by Wood and Tauc [25] according to the following equation,

$$(h\nu\alpha)\alpha(h\nu - E_g)^n \quad (5)$$

where ' $\alpha$ ' is the absorbance, ' $h$ ' is the Planck constant, ' $\nu$ ' is the frequency, ' $E_g$ ' is the optical energy band gap and ' $n$ ' is a constant associated to the different types of electronic transitions ( $n = 1/2, 2, 3/2$  or  $3$  for direct allowed, indirect allowed, direct forbidden and indirect forbidden transitions, respectively). ' $E_g$ ' value for  $\text{ZnTiO}_3$  ceramic is 3.6 eV which is well agreement with the literature.

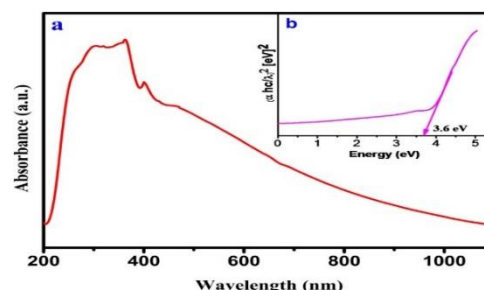


Fig. 4(a) UV-Vis spectrum (b) Optical energy band gap of  $\text{ZnTiO}_3$  nanocrystals

#### 3.5 Morphological Analysis

Fig. 5 shows FE-SEM image of  $\text{ZnTiO}_3$  nanocrystals. Micrograph reveals that the particles are nearly spherical in shape, has uniform size and distribution. The particles are highly agglomerated due to sintering of particles during calcination. TEM image of  $\text{ZnTiO}_3$  nanocrystals (Fig. 6(a)) shows that the particles obtained are in nano regime and has average particle size  $\sim 5\text{ nm}$ . HR-TEM image (Fig. 6(b)) shows that the  $\text{ZnTiO}_3$  nanocrystals are highly crystalline with lattice spacing of 0.23 nm.

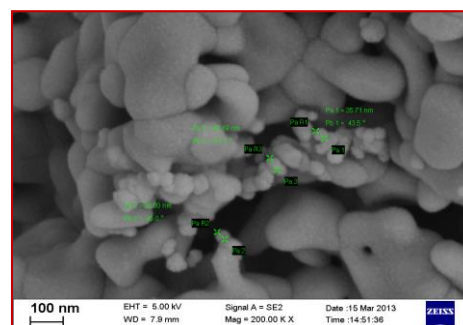


Fig. 5 FE-SEM micrograph  $\text{ZnTiO}_3$  nanocrystals

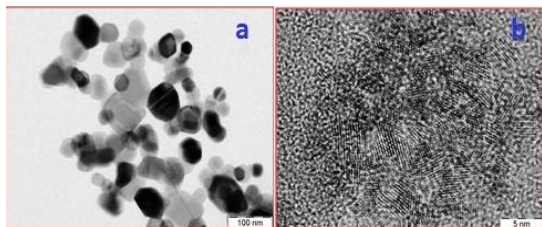


Fig. 6 (a) TEM (b) HRTEM micrographs ZnTiO<sub>3</sub> nanocrystals

### 3.6 Photoluminescence (PL) Studies

The PL emission spectrum of ZnTiO<sub>3</sub> nanocrystals is shown in Fig. 7. It shows that upon 345 nm excitation, a series of emission bands ranging from UV to green region are observed, and the bands were centered at 412, 450, 461, 492 and 542 nm. Since Zn<sup>2+</sup> itself is non-luminous and the observed luminescence from ZnTiO<sub>3</sub> nanocrystals must be due to non-stoichiometry created by the oxygen deficiency in the system, which is expected to arise when ZnTiO<sub>3</sub> nanocrystals forms in carbon rich ambient [26]. In the emission spectra, the broad emission peak at 412 nm in UV region is attributed to radiative recombination of photo-generated hole with an electron occupying the oxygen vacancy [27]. Emission band centered at 461 nm is attributed to recombination of a delocalized electron close to the conduction band with a single charged state of surface oxygen vacancy [28]. The emission band at 484 nm can be attributed to self-trapped excitation luminescence [29].

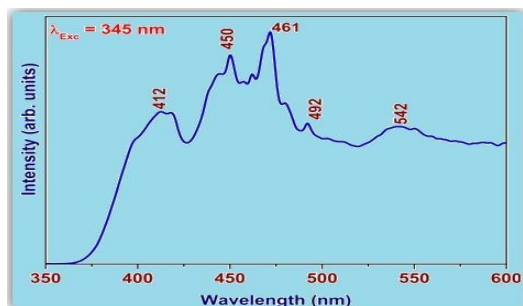


Fig. 7 PL emission spectrum of ZnTiO<sub>3</sub> nanocrystals

## 4. Conclusion

The ZnTiO<sub>3</sub> nanocrystals were successfully synthesized by carbothermal method and studied its characteristics. The PL emission in this particular study is ascribed to the presence of amorphous carbon and it is independent of the excitation wavelength.

## Acknowledgements

The authors R.S. Raveendra and P.A. Prashanth thank the principal and management of Sai Vidya Institute of Technology, Bengaluru for their constant encouragement.

## References

[1] H. Liu, J. Xu, Y. Li, Y. Li, Aggregate nanostructures of organic molecular materials, *Acc. Chem. Res.* 43 (2010) 1496-1508.  
 [2] C.T. Kresge, M.E. Leonowicz, W.J. Roth, J.C. Vartuli, J.S. Beck, Ordered mesoporous molecular sieves synthesized by a liquid-crystal template mechanism, *Nature* 359 (1992) 710-712.

[3] J. Sauer, S. Kaskel, M. Janicke, F. Scheuth, 29-P-17-Zirconia nanoparticles in ordered mesoporous material SBA-15, *Stud. Surf. Sci. Catal.* 135 (2001) 315-319.  
 [4] C.A. Morris, M.L. Anderson, R.M. Stroud, C.I. Merzbacher, D.R. Rolison, Silica sol as a nanogluue: flexible synthesis of composite aerogels, *Sci.* 284 (1999) 622-624.  
 [5] LI Mengting, JIAO Baoxiang, Synthesis and photoluminescence properties of ZnTiO<sub>3</sub>:Eu<sup>3+</sup> red phosphors via sol-gel method, *J. Rare Earth* 33 (2015) 231-238.  
 [6] Y.C. Jia, H. Qiao, Y.H. Zheng, N. Guo, H.P. You, Synthesis and photoluminescence properties of Ce<sup>3+</sup> and Eu<sup>2+</sup> activated Ca<sub>7</sub>Mg(SiO<sub>4</sub>)<sub>4</sub> phosphors for solid state lighting, *Phys. Chem. Chem. Phys.* 14 (2012) 3537-3542.  
 [7] S. Pimputkar, J.S. Speck, S.P. DenBaars, S. Nakamura, Prospects for LED lighting, *Nat. Photonics* 3 (2009) 180-182.  
 [8] T. Ogi, A.B.D. Nandiyanto, W.N. Wang, F. Iskandar, K. Okuyama, Direct synthesis of spherical YAG: Ce phosphor from precursor solution containing polymer and urea, *Chem. Engg. J.* 210 (2012) 461-466.  
 [9] A. Herrmann, A. Simon, C. Russel, Preparation and luminescence properties of Eu<sup>2+</sup>-doped BaSi<sub>2</sub>O<sub>5</sub> glass-ceramics, *J. Lumin.* 132 (2012) 215-219.  
 [10] X.G. Lu, K. Zhao, Enhanced photoluminescence of Eu<sup>3+</sup>-activated calcium molybdate system by co-doping Li<sup>+</sup> and Si<sup>4+</sup> ions, *Opt. Mater.* 34 (2012) 1926-1929.  
 [11] M.M. Haque, H.I. Lee, D.K. Kim, Luminescent properties of Eu<sup>3+</sup>-activated molybdate-based novel red-emitting phosphors for LEDs, *J. Alloys Compd.* 481 (2009) 792-796.  
 [12] Y.B. Chen, K.W. Cheah, M.L. Gong, Low temperature quenching and high efficiency Tm<sup>3+</sup>, La<sup>3+</sup> or Tb<sup>3+</sup> co-doped CaSc<sub>2</sub>O<sub>4</sub>:Ce<sup>3+</sup> phosphors for light-emitting diodes, *J. Lumin.* 131 (2011) 1770-1775.  
 [13] X.G. Zhang, L.Y. Zhou, M.L. Gong, High-brightness Eu<sup>3+</sup> doped Ca<sub>3</sub>(PO<sub>4</sub>)<sub>2</sub> red phosphor for NUV light-emitting diodes application, *Opt. Mater.* 35 (2013) 993-997.  
 [14] H.W. Yao, R.B. Feng, Preparation and characterization of sol-gel derived ZnTiO<sub>3</sub> nanocrystal, *Min. Saf. Environ. Prot.* 28 (2001) 20-24.  
 [15] S.F. Wang, M.K. Leu, F. Gu, C.F. Song, D. Xu, et al, Photoluminescence characteristics of Pb<sup>2+</sup> ion in sol-gel derived ZnTiO<sub>3</sub> nanocrystals, *Inorg. Chem. Commun.* 6 (2003) 185-188.  
 [16] S.F. Wang, F. Gu, M.K. Le, C.F. Song, Photoluminescence of sol-gel derived ZnTiO<sub>3</sub>:Ni<sup>2+</sup> nanocrystals, *Chem. Phys. Lett.* 373 (2003) 223-227.  
 [17] R.S. Raveendra, P.A. Prashanth, R. Hari Krishna, N.P. Bhagya, B.M. Nagabhushana, et al, Synthesis, structural characterization of nano ZnTiO<sub>3</sub> ceramic: an effective azo dye adsorbent and antibacterial agent, *J. Asian Ceram. Soc.* 2 (2014) 357-365.  
 [18] S.J. Yun, Y.S. Kim, S.K. Park, Fabrication of CaS: Pb blue phosphor by incorporating dimeric Pb<sup>2+</sup> luminescent centers, *Appl. Phys. Lett.* 78 (2001) 721-723.  
 [19] H.T. Kim, J.D. Byun, Y. Kim, Microstructure and microwave dielectric properties of modified zinc titanates, *Mater. Res. Bull.* 33 (1998) 963-973.  
 [20] P.A. Prashanth, R.S. Raveendra, R.H. Krishna, N.P. Bhagya, S. Ananda, et al, Synthesis, characterizations, antibacterial and photoluminescence studies of solution combustion-derived α-Al<sub>2</sub>O<sub>3</sub> nanoceramic, *J. Asian Ceram. Soc.* 3 (2015) 345-351.  
 [21] K.C. Patil, S.T. Aruna, T. Mimani, Combustion synthesis: an update, *Curr. Opin. Sol. Stat. Mater. Sci.* 6 (2002) 507-512.  
 [22] R.S. Raveendra, P.A. Prashanth, B.M. Nagabhushana, Study on the effect of fuels on phase formation and morphology of combustion derived α-Al<sub>2</sub>O<sub>3</sub> and NiO nanomaterials, *Adv. Mater. Lett.* 7 (2016) 216-220.  
 [23] P. Klug, L.E. Alexander, X-ray diffraction procedure, Wiley, New York, 1954.  
 [24] Y.L. Chai, Y.S. Chang, G.J. Chen Y.J. Hsiao, The effects of heat-treatment on the structure evolution and crystallinity of ZnTiO<sub>3</sub> nano-crystals prepared by Pechini process, *Mater. Res. Bull.* 43 (2008) 1066-1073.  
 [25] Tauc, In. F. Abeles (Ed.), Optical properties of solids, North-Holland, Amsterdam, 1970.  
 [26] R. Hari Krishna, B.M. Nagabhushana, H. Nagabhushana, R.P.S. Chakradhar, R. Sivaramakrishna, et al, Auto-ignition based synthesis of Y<sub>2</sub>O<sub>3</sub> for photo and thermo-luminescent applications, *J. Alloys Comp.* 585 (2014) 129-137.  
 [27] B. Umesha, B. Eraiah, H. Nagabhushana, B.M. Nagabhushana, G. Nagaraja, et al, Synthesis and characterization of spherical and rod like nano crystalline Nd<sub>2</sub>O<sub>3</sub> phosphors, *J. Alloys Comp.* 509 (2011) 1146-1151.  
 [28] C. Hu, H. Liu, W. Dong, Y. Zhang, G. Bao, et al, La(OH)<sub>3</sub> and La<sub>2</sub>O<sub>3</sub> nanobelts-synthesis and physical properties, *Adv. Mater.* 19 (2007) 470-474.  
 [29] Y. Zhang, K. Han, T. Cheng, Z. Fang, Synthesis, characterization, and photoluminescence property of LaCO<sub>3</sub>OH microspheres, *Inorg. Chem.* 46 (2007) 4713-4717.